*Progress In Electromagnetics Research Letters, Vol. 46, 73–78, 2014*

# A Broadband Flexible Metamaterial Absorber Based on Double Resonance

**Hong-Min Lee***

**Abstract**—We present a broadband microwave metamaterial (MM) absorber, the unit cell of which consists of a lumped-resistor-loaded electric-inductive-capacitive (ELC) resonator and a cut-wire on the same side of a flexible polyimide substrate. In contrast to the common MM absorber, the metallic pattern layer of the proposed structure is placed parallel to the direction of propagation of the incident wave in order to reduce the radar cross-section (RCS) at frequencies other than the targeted frequency bands. Our experiments show that the proposed absorber exhibits a peak absorption rate of 92% and 93% at 8.6 GHz and 13.4 GHz, respectively, and 88% of the full-width at half-maximum (FWHM) bandwidth is achieved.

## 1. INTRODUCTION

Recently, the absorber technology has seen several advancements in the use of artificially structured metamaterials (MMs) for the microwave terahertz, and optical frequency regimes [1–3]. The configuration of the previously reported MM absorbers can be categorized into two types: absorber with metallic backing plate and metallic backplane-less absorbers. Most of the MM absorbers, to avoid power transmission on the other side of the absorber, are equipped with a metallic backing plate [4–8]. However, the presence of backing plates may be disadvantageous in stealth and camouflage applications [9]. If the object to be hidden is composed of a nonmetallic material, the metallic backing plate of the MM absorber can be considered as a material object at frequencies other than the targeted absorption frequency bands. The configuration of the previously reported metallic backplane-less MM absorbers involves the realization of both the metallic patterns with the negative real parts of the permittivity and permeability. The two metallic pattern layers separated by a dielectric spacer are placed orthogonal to the electromagnetic (EM) wave propagation direction [10–14]. In this case the radar cross-section (RCS) of the metallic pattern expands at frequencies other than the targeted frequency bands. Therefore, there is a need for a metallic pattern layer of the MM absorber to be designed in parallel to the EM wave propagation direction, to avoid this problem. This type of MM absorber configuration was first demonstrated by employing a resistive sheet and multiple split-ring resonators (SRRs) designed on the basis of resonant magnetic inclusion [9]. However, the absorber requires a resistive sheet designed at a certain distance from the MM slab in order to match the MM impedance to that of free space. In our previous study, an MM absorber structure whose metallic pattern layers are placed parallel to the EM wave propagation direction was introduced [15, 16]. Although this structure serves as an MM absorber in the microwave frequency region, the absorption bandwidth of this MM absorber is quite narrow. This narrow bandwidth characteristic limits absorber applications. In addition, the absorber cannot be used on irregular surfaces. In this work, a compact flexible MM absorber at microwave frequencies is presented by employing a flexible polyimide and silicone rubber substrate.

*Received 18 March 2014, Accepted 2 May 2014, Scheduled 19 May 2014*
* Corresponding author: Hong-Min Lee (hmlee@kyonggi.ac.kr).
The author is with the Department of Electronic Engineering, Kyonggi University, Suwon, Republic of Korea.

## 2. LUMPED-RESISTORS-LOADED ELC RESONATOR

Figure 1 shows the two ELC resonators with different incident EM field orientations. The ELC resonators comprise a single metallic pattern layer etched on a Rogers R4003C dielectric substrate, which has a relative dielectric constant $\varepsilon_r$ of 3.37, loss tangent $\delta$ of 0.003, and thickness $t$ of 1.5 mm. Copper, with a conductivity $\sigma$ of $5.8 \times 10^7$ S/m, is used for designing the metallic patterns. These layers are illuminated with a plane wave propagating in the $k$ direction, and for this, two different illumination polarizations are considered: perpendicular polarization (case 1), where the magnetic field $H$ is parallel to the ELC resonator, and the electric field $E$ is coupled to the capacitive element, as shown in Figure 1(a); and parallel polarization (case 2), where the magnetic field $H$ is normal to the ELC resonator, and the electric field $E$ is coupled to the capacitive element, as shown in Figure 1(b). Computer simulations are carried out using the commercial solver of CST Microwave Studio. This program simulates a single ELC resonator under appropriate periodic boundary conditions.

The effective permittivity $\varepsilon_{eff}$ and permeability $\mu_{eff}$ of the artificial material are expressed in terms

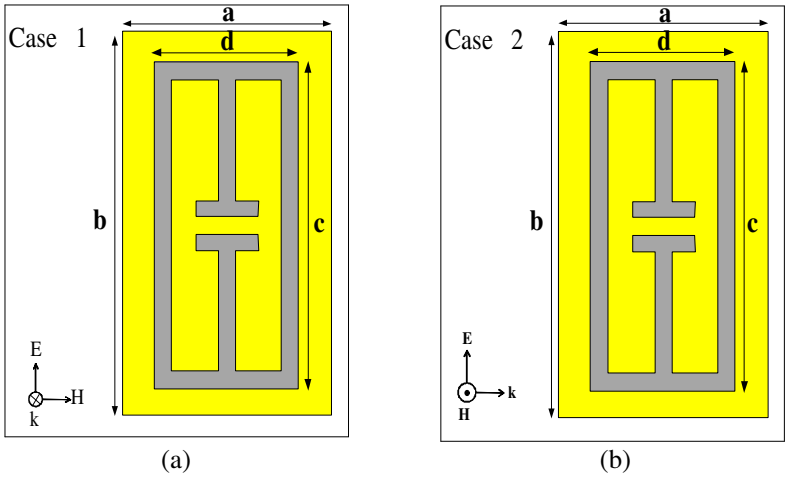


**Figure 1.** Two ELC resonators with different incident EM field orientations: (a) perpendicular polarization and (b) parallel polarization. The geometric dimensions of two ELC resonators are: $a = 3.5$ mm. $b = 9.2$ mm, $c = 6.9$ mm, $d = 2.5$ mm.

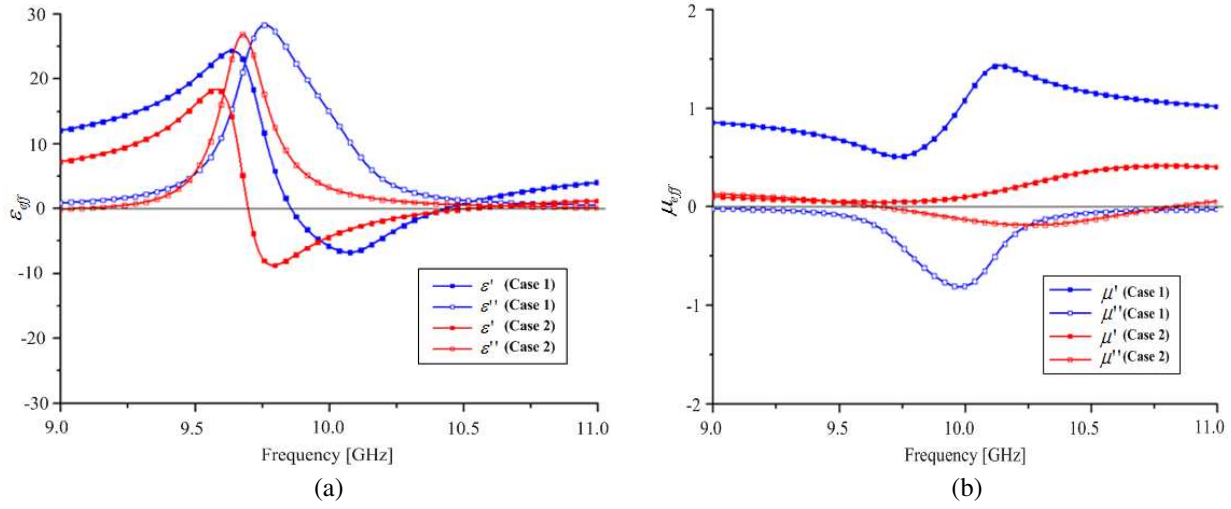


**Figure 2.** Retrieved effective medium parameters for two different orientations of the two ELC resonators: (a) effective permittivity, (b) effective permeability.

of the scattering parameters by conventionally retrieving the relevant information from the scattering parameters of the unit cell. The extracted effective permittivity $\varepsilon_{eff}(= \varepsilon' + j\varepsilon'')$ and permeability $\mu_{eff}(= \mu' + j\mu'')$ of the two ELC resonators over a frequency range of 9–11 GHz are plotted as shown in Figures 2(a) and (b), respectively. The ELC resonator mostly used in the literature is involved in coupling the fundamental mode to the external field with perpendicular polarization (case 1), as shown in Figure 1(a). In this field orientation of the ELC, the capacitive element couples strongly to the electric field, and the inductive loop does not. As a result, there is a strong electric resonance with the real part of the effective permittivity ranging from nearly 25 down to −8 (case 1), as shown in Figure 2(a), and there is a small anti-resonance at magnetic response in effective permeability, as shown in Figure 2(b). The ELC resonator used in this study has a different external field orientation which is named parallel polarization (case 2), as shown in Figure 1(b). This type of the external field orientation for the ELC resonator was not shown in the literature. In both the cases, there are Lorentzian types of strong electric resonances in effective permittivity, owing to the electric coupling, as shown in Figure 2(a). However, there are no significant Lorentzian types of magnetic resonances in effective permeability, as shown in Figure 2(b).

## 3. MM ABSORBER UNIT CELL DESIGN WITH LUMPED-RESISTORS-LOADED ELC RESONATOR AND WIRE-STRIP

We have designed a composite MM absorber that employs three layers, two flexile dielectric layers and a metallic layer, as shown in Figure 3(a). The top layer consists of an electric-inductive-capacitive (ELC) resonator [17] and a cut-wire on the same side of a polyimide substrate (second layer), which has a relative dielectric constant $\varepsilon_r$ of 3.5, and thickness $t_1$ of 125 µm.

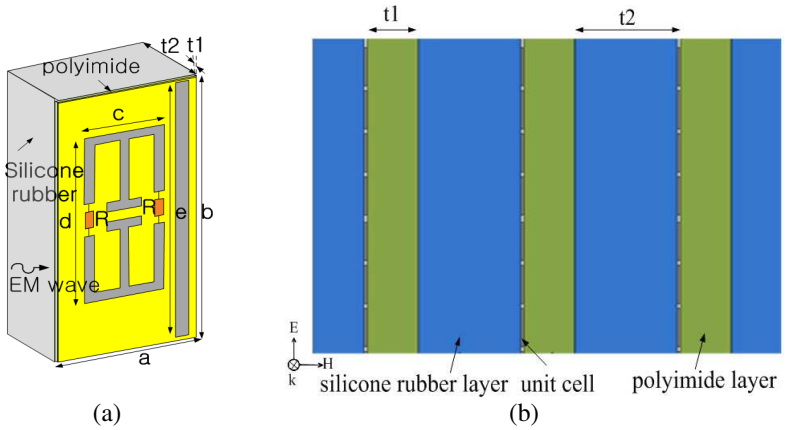


**Figure 3.** Schematics of (a) optimum single-cell absorber parameters of $a = 4.3\,\text{mm}$, $b = 9.2\,\text{mm}$, $c = 2.5\,\text{mm}$, $d = 6.9\,\text{mm}$, $e = 9\,\text{mm}$, $t_1 = 125\,\mu\text{m}$, $t_2 = 4\,\text{mm}$, $R = 570\,\Omega$ and (b) front view of the planar absorber structure with periodic array of the vertically aligned unit cells.

The two lumped resistors are loaded in the inductive arms of an ELC resonator in order to reduce the quality (Q) factor of the resonator. A silicone rubber layer, which has a relative dielectric constant $\varepsilon_r$ of 2.7, loss tangent $\delta$ of 1.5, and thickness $t_2$ of 4 mm, is used at the bottom as a supporting substrate. In the simulations carried out by us, the incident EM wave illuminates the proposed MM absorber placed parallel to the direction of propagation of the incident wave, with the magnetic field $H$ normal to the ELC resonator and the electric field $E$ coupled to the capacitive element, as shown in Figure 3(b). We obtain two resonant modes near frequencies of 8.4 and 13.6 GHz. Figure 4 shows the simulated magnetic field distribution and the main surface current directions at the two resonant frequencies. Near the resonant frequency of 8.4 GHz, the cut-wire provides the electric response by coupling strongly to the incident electric field while the circular surface current that concentrates on the left SRR in the ELC resonator provides a magnetic response, as shown in Figure 4(a).

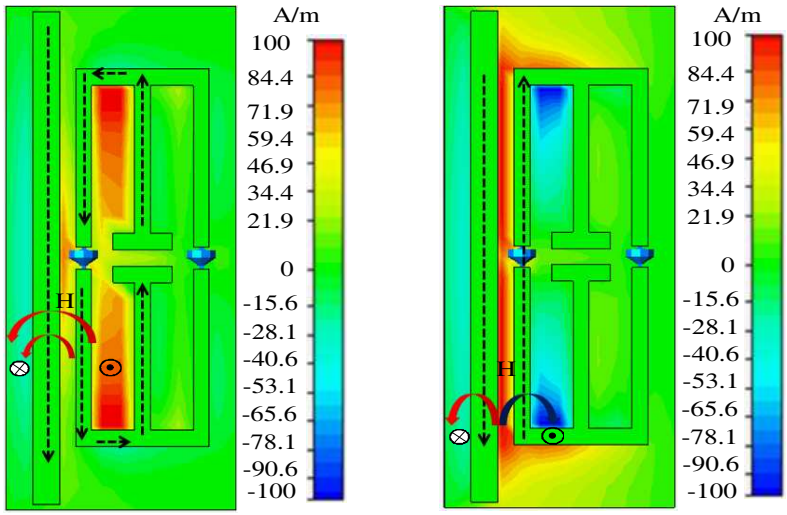


**Figure 4.** Simulated results of (a) the magnetic field distribution for the MM absorber unit cell at the first resonant frequency of 8.4 GHz and (b) the second resonant frequency of 13.6 GHz, respectively. The black dots arrows indicate the main surface current directions on the metallic patterns.

However, near the resonant frequency of 13.6 GHz, magnetic coupling is achieved by antiparallel currents in the cut-wire and the inductive arm of the left SRR in the ELC resonator, as shown in Figure 4(b). These antiparallel currents create a magnetic response [18] while the electric response arises from surface-plasmon resonance in the cut-wire.

## 4. MEASUREMENT RESULTS

The fabricated MM absorber sample strip is shown in Figure 5(a). The sample was etched on a 125 μm-thick polyimide substrate using standard photolithography techniques. A 4 mm-thick silicone rubber was used as a supporting substrate. The lumped resistors (resistance $R = 570\,\Omega$, 1005-type thick film with a size of $1.0 \times 0.5$ mm) were then loaded on the inductive arms of the ELC resonators by applying the surface-mount soldering technology. An appropriately designed composite absorber sample was fabricated with a planar array of $47 \times 33$ unit cells, as shown in Figure 5(b). The total size of the fabricated planar MM absorber sample was 194 mm × 303 mm × 4.3 mm. The plots of the calculated


**Figure 5.** (a) Photograph of the fabricated prototype flexible absorber strip sample, (b) planar arrayed MM absorber strips and (c) the experimental results of absorption rate of the composite MM absorber at normal incidence.

and measured frequency-dependent absorption rates using the measured magnitudes of the $S_{11}$ and $S_{21}$ parameters of the planar arrayed unit cells are shown in Figure 5(c).

The results show that the experimental peak absorption rate is slightly lower than that demonstrated by the simulated results. Our experiments show that the proposed absorber exhibits a peak absorption of 92% and 93% at 8.6 GHz and 13.4 GHz, respectively, and the full width at full-width half-maximum (FWHM) bandwidth is around 9.7 GHz. In addition, the measured peak absorption curve as a function of different incident angles for the TE and TM polarizations of the EM waves is plotted in Figure 6. For both TE and TM polarizations, with increasing angle of incidence, the overall peak absorption slightly decreases. However, the peak absorption rate remains above 88% (for TE case) and 84% (for TM case), irrespective of the incident angles up to 45°. The results show that the proposed metamaterial absorber operates quite well for both TE and TM polarizations over a large range of angles of incidence.

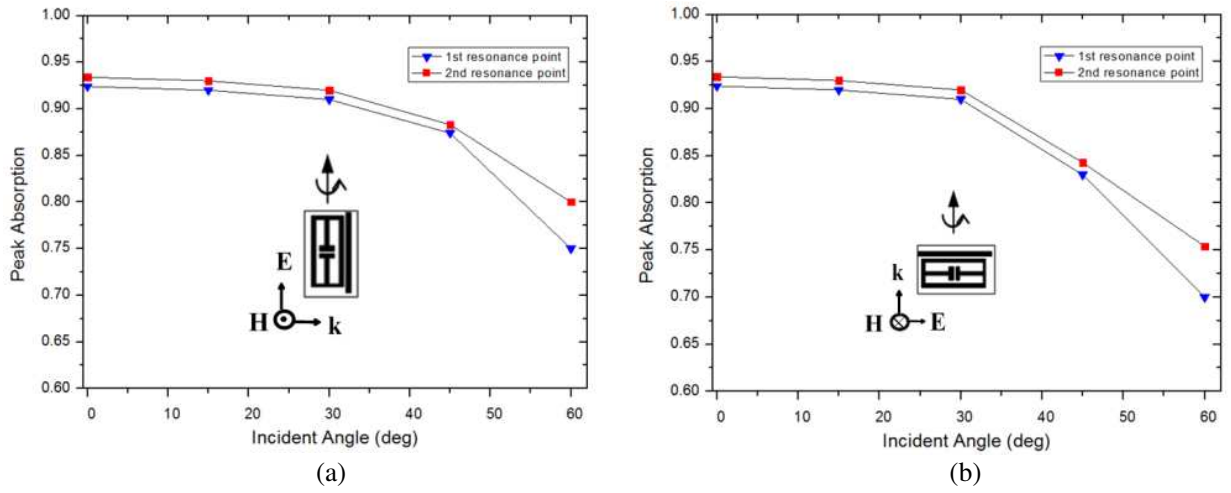


**Figure 6.** Measured peak absorption curve as a function of different incident angles for (a) TE and (b) TM incidence.

## 5. CONCLUSIONS

We have designed, simulated, and experimentally verified a broadband MM absorber configuration. A metallic pattern layer of the proposed absorber is designed parallel to the incident wave propagation direction, and it is fabricated on a flexible substrate. The proposed design has several advantages: 1) It can be used on non-planar surfaces. 2) This MM absorber achieves a broader bandwidth compared with previous designs. 3) The metallic pattern layer of the proposed structure is placed on the same side of the polyimide substrate. A precise alignment between the layers of the metallic patterns is not required owing to the one-layer design.

## REFERENCES

1. Landy, N. I., S. Sajuyigbe, J. J. Mock, D. R. Smith, and W. J. Padilla, "Perfect metamaterial absorber," *Phys. Rev. Lett.*, Vol. 100, 274021–274024, 2008.
2. Tao, H., N. I. Landy, C. M. Bingham, X. Zang, R. D. Averitt, and W. J. Padilla, "A metamaterial absorber for the terahertz regime: Design, fabrication and characterization," *Optic Express*, Vol. 16, 7181–7188, 2008.
3. Alici, K. B., A. B. Turhan, C. M. Soukoulis, and E. Ozbay, "Optically thin composite resonant absorber at the near-infrared band: A polarization independent and spectrally broadband configuration," *Optic Express*, Vol. 19, No. 15, 14260–14267, 2011.

4. Tao, H., C. M. Bingham, D. Pilon, K. Fan, A. C. Strkwerda, D. Shrekenhammer, W. J. Padilla, X. Zhang, and R. D. Averitt, "A dual band terahertz metamaterial absorber," *J. Appl. Phys. D*, Vol. 43, 225102–225106, 2010.
5. Li, M., H.-L. Yang, X.-W. Hou, Y. Tian, and D.-Y. Hou, "Perfect metamaterial absorber with dual bands," *Progress In Electromagnetics Research*, Vol. 108, 37–49, 2010.
6. Lee, J. and S. Lim, "Bandwidth-enhanced and polarization-insensitive metamaterial absorber using double resonance," *Electron. Lett.*, Vol. 47, 8–9, 2011.
7. Cheng, Y., H. Yang, Z. Cheng, and N. Wu, "Perfect metamaterial absorber based on a split-ring-cross resonator," *J. Appl. Phys. A*, Vol. 102, 99–103, 2010.
8. He, X.-J., Y. Wang, J. Wang, T. Gui, and Q. Wu, "Dual-band terahertz metamaterial absorber with polarization insensitivity and wide incident angle," *Progress In Electromagnetics Research*, Vol. 115, 381–397, 2011.
9. Bilotti, F., A. Toscano, K. B. Alici, E. Ozbay, and L. Vegini, "Design of miniaturized narrowband absorbers based on resonant-magnetic inclusions," *IEEE Trans. on Electromagnetic Compatibility*, Vol. 53, 63–72, 2011.
10. Cheng, Y. and H. Yang, "Design, simulation, and measurement of metamaterial absorber," *Microwave Opt. Tech. Lett.*, Vol. 52, 877–880, 2010.
11. Tao, H., C. M. Bingham, D. Pilon, K. Fan, A. C. Strikwerda, D. Shrekenhamer, W. J. Padilla, X. Zhang, and R. D. Averitt, "A dual band terahertz metamaterial absorber," *J. of Phys. D: Appl. Phys.*, Vol. 43, 225102–225106, 2010.
12. Shen, X., T. J. Cui, J. Zhao, H. F. Ma, W. X. Jiang, and H. Li, "Polarizationindependent wide-angle triple-band metamaterial absorber," *Optic Express*, Vol. 19, 9401–9407, 2011.
13. Li, H., L. H. Yuan, B. Zhou, X. P. Shen, Q. Cheng, and T. J. Cui, "Ultrathin multiband gigahertz metamaterial absorbers," *J. Appl. Phys.*, Vol. 110, 0149091–0149098, 2011.
14. Zhu, B., Z. Wang, C. Huang, Y. Feng, J. Zhao, and T. Jiang, "Polarization insensitive metamaterial absorber with wide incident angle," *Progress In Electromagnetics Research*, Vol. 101, 231–239, 2010.
15. Lee, H.-M. and H.-S. Lee, "A dualband metamaterial absorber based with resonantmagnetic structures," *Progress In Electromagnetics Research Letters*, Vol. 33, 1–12, 2012.
16. Lee, H.-M. and H.-S. Lee, "A metamaterial based microwave absorber composed of coplanar electric-field-coupled resonator and wire array," *Progress In Electromagnetics Research C*, Vol. 34, 111–121, 2013.
17. Schurig, D., J. J. Mock, and D. R. Smith, "Electric-field-coupled resonators for negative permittivity metamaterials," *Appl. Phys. Lett.*, Vol. 88, 0411091–0411093, 2006.
18. Zhou, J., E. N. Economon, T. Koschny, and C. M. Soukoulis, "Unifying approach to left-handed material design," *Optic Express*, Vol. 31, 3620–3622, 2006.